Effect of next-nearest neighbor hopping on the spin dynamics in antiferromagnets

Dirk K. Morr
University of Illinois at Urbana-Champaign, Loomis Laboratory of Physics
1110 W. Green St., Urbana, Il, 61801
(February 1, 2008)

Recently, inelastic neutron scattering (INS) experiments on the insulating parent compounds of high-T_c materials were analyzed to extract the value of the superexchange constant J. Starting point of the analysis was the nearest-neighbor Heisenberg model. Motivated by recent ARPES experiments, we consider the effects of a next-nearest neighbor hopping, t' in the strong coupling limit of the spin-density wave formalism, where it leads to an antiferromagnetic exchange $J' > 0$ between next-nearest neighbor spins. We show that a finite J' (a) changes the spin-wave velocity and thus the value of J extracted from the INS data, yielding almost identical values for J in La_2CuO_4 and $YBa_2Cu_3O_{6.15}$, and (b) leads to a considerable change in the high-frequency spin-dynamics. Finally, we calculate the $1/S$ quantum corrections in the presence of J' and discuss their relevance for the INS data.

The strong evidence for antiferromagnetic fluctuations as the source of the pairing mechanism in the high-T_c materials [1,2] makes it important to understand the variation of the energy scale J of these fluctuations in different compounds. The materials for which J can be easily determined are the insulating parent compounds of the high-T_c materials. Here, the energy scale J of the spin-wave mode can be extracted from Raman [3] or inelastic neutron scattering (INS) experiments [4]. Recently, INS experiments [4,5] on the insulating parent compounds La_2CuO_4, Nd_2CuO_4, Pr_2CuO_4 and $YBa_2Cu_3O_{6.15}$, which possess an antiferromagnetic ground state, were analyzed using the Heisenberg model with nearest-neighbor exchange J. Combining the experimentally measured spin-wave velocity c_{sw} with the theoretical expression $c_{sw} = \sqrt{2}J$ of the Heisenberg model, values of J were obtained which range from $J \approx 125$ meV in $YBa_2Cu_3O_{6.15}$ to $J \approx 160$ meV in Nd_2CuO_4. However, various theoretical studies [6,7] of angle-resolved photoemission (ARPES) experiments [8] as well as band-structure calculations [9] suggest, that the experimentally measured fermionic dispersion provides evidence for a finite next-nearest neighbor hopping, t', with $t'/t \approx -0.25$ for La_2CuO_4 and $t'/t \approx -0.45$ for $YBa_2Cu_3O_{6.15}$. In the strong coupling limit of the insulating parent compounds, t' leads to an antiferromagnetic coupling $J' > 0$ between next-nearest neighbors spins which changes c_{sw} and in turn the value of J extracted from the INS data.

In this communication we investigate the effect of J' on the spin dynamics in single and double-layer compounds. We show that J' not only changes the spin-wave velocity but also the spin-dynamics at higher frequencies. We reanalyze the INS data and demonstrate that J extracted in the presence of a finite J' is actually larger than previously assumed [4]. In particular, we obtain almost identical values for J in La_2CuO_4 and $YBa_2Cu_3O_{6.15}$. Furthermore, we compute $1/S$ (quantum) corrections [10,11] for various physical quantities. These corrections increase with increasing J', which is expected since $J' > 0$ frustrates the system and should thus lead to an increase of quantum fluctuations. Finally, we discuss our results in the context of the experimentally observed strong renormalization of the transverse spin susceptibility.

We study the effects of t' on the spin dynamics by computing the transverse susceptibility within the spin-density wave (SDW) formalism at $T = 0$. Since this formalism is thoroughly described in the literature [12], we will outline it only briefly. For simplicity we first consider the case of a single-layer compound. The starting point for the description of the CuO_2 planes in the insulating parent compounds is the effective 2D one-band Hubbard model [2,13] at half filling, given by

$$\mathcal{H} = -\sum_{i,j} t_{i,j} c^\dagger_{i,\alpha} c_{j,\alpha} + U \sum_i c^\dagger_{i,\uparrow} c_{i,\uparrow} c^\dagger_{i,\downarrow} c_{i,\downarrow} \ . \qquad (1)$$

Here α is the spin index and $t_{i,j}$ is the hopping integral which we assume to act between nearest and next-nearest neighbors (t and t', respectively). In the strong coupling limit, $t \ll U$ the ground state of the Hubbard model is antiferromagnetically ordered, and one can use the antiferromagnetic long range order parameter $\langle S_z \rangle = \sum_k \langle c^\dagger_k c_{k+Q} \rangle$ to decouple the interaction term in Eq.(1). Diagonalizing then the quadratic form by means of a unitary transformation one obtains two electronic bands for the conduction and valence fermions whose mean-field energy dispersions are given by

$$E^{c,v}_k = \pm \sqrt{(\epsilon^-_k)^2 + \Delta^2} + \epsilon^+_k \ , \qquad (2)$$

where $\epsilon^\pm_k = (\epsilon_k \pm \epsilon_{k+Q})/2, \Delta = U\langle S_z \rangle$, and

$$\epsilon_k = -2t(\cos k_x + \cos k_y) - 4t' \cos k_x \cos k_y - \mu \ . \qquad (3)$$

Here $E^{c,v}_k$ is the dispersion of the conduction and valence fermions, respectively, ϵ_k is the dispersion of free fermions, and μ is the chemical potential.

Next we calculate the transverse susceptibility which is defined by

$$\chi^{+-}(\mathbf{q},\mathbf{q}',t) = i\langle T S^+_{\mathbf{q}}(t) S^-_{-\mathbf{q}'}(0)\rangle \ , \tag{4}$$

where the spin operators are given by

$$\mathbf{S_q} = \frac{1}{2}\sum_k c^\dagger_{\mathbf{k+q},\alpha}\sigma_{\alpha,\beta}c_{\mathbf{k},\beta} \ , \tag{5}$$

and σ are the Pauli matrices. Within the RPA approximation χ^{+-} is given by an infinite series of fermionic bubble diagrams [12], with fermions obeying the dispersion given in Eq.(2). Since the susceptibilities with zero momentum transfer (i.e. $\mathbf{q}' = \mathbf{q}$) and with momentum transfer $\mathbf{Q} = (\pi,\pi)$ (i.e. $\mathbf{q}' = \mathbf{q}+\mathbf{Q}$) are finite, the evaluation of χ^{+-} reduces to a (2×2) algebraic equation. One obtains after some tedious algebra (for S=1/2)

$$\begin{aligned}
\chi^{+-}(\mathbf{q},\mathbf{q},\omega) &= \frac{-2J\Big[1-\nu_{\mathbf{q}}-\frac{J'}{J}\Big(1-cos(q_x)cos(q_y)\Big)\Big]}{\omega^2-\omega^2(\mathbf{q})+i\delta}, \\
\chi^{+-}(\mathbf{q},\mathbf{q}+\mathbf{Q},\omega) &= -\frac{\omega}{\omega^2-\omega^2(\mathbf{q})+i\delta},
\end{aligned} \tag{6}$$

where $J = 4t^2/U$, $J' = 4(t')^2/U$ are the superexchange constants and $\nu_{\mathbf{q}} = (cos(q_x)+cos(q_y))/2$. The magnon dispersion $\omega(\mathbf{q})$ is given by

$$\omega(\mathbf{q}) = 2J\sqrt{\Big[1-\frac{J'}{J}(1-cos(q_x)cos(q_y))\Big]^2-\nu^2_{\mathbf{q}}} \ . \tag{7}$$

A comparison of Eq.(7) with the mean-field magnon dispersion of the Heisenberg model with next-nearest neighbor exchange J' shows, as expected, that in the strong coupling limit t' leads to an antiferromagnetic coupling $J' > 0$.

From Eq.(6) we see that the terms $\sim J'$ vanish in the limit $\mathbf{q} = 0$, which means that the static, uniform susceptibility $\chi_\perp = 1/8J$ is not affected by J'. In contrast, J' changes the spin-wave velocity c_{sw}, which is given by

$$c_{sw} = \sqrt{2}J\sqrt{1-2\frac{J'}{J}} \ . \tag{8}$$

Using the hydrodynamical relation $\rho_s = c^2_{sw}\chi_\perp$ we obtain for the spin stiffness $\rho_s = J(1-2J'/J)/4$ which was previously reported in Ref. [7].

We now discuss our results in the light of the available INS data. In Fig. 1 we present a fit of the magnon dispersion Eq.(7) for $t' = -0.3t$ (solid line) to the experimental data on La_2CuO_4 from Ref. [14]. This fit yields $J = 166(\pm 6)$ meV, a value approximately 6% larger than in Ref. [4], and $J' = 15 \pm 1$ meV. For comparison, we also present a fit of the magnon dispersion with $t' = 0$ (dashed line). Note, that only the functional form of the high-frequency part of the dispersion is changed by J'. Here, J' removes the degeneracy along the boundary of the magnetic Brillouin zone (MBZ) ($(0,\pi)$ to $(\pi,0)$ direction), and gives rise to a local maximum along the $(0,\pi)$ to (π,π) direction (indicated by an arrow). It is, however, questionable whether INS experiments are sensitive enough to detect this difference since the effect is only of the order of 10%, and thus might very well lie within the experimental errorbars.

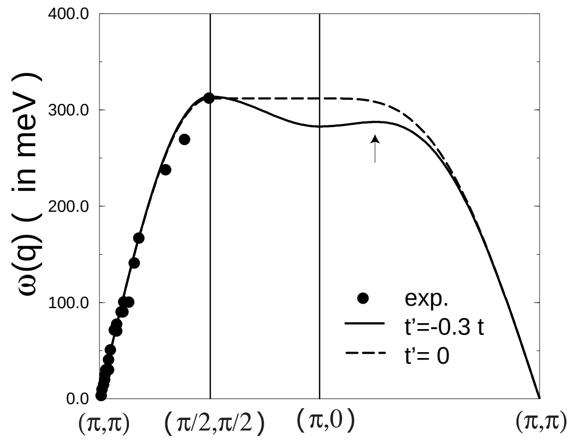

FIG. 1. Fit to the experimental magnon dispersion for $t' = -0.3t$ (solid line) and $t' = -0.0$ (dashed line). The experimental data are taken from Ref. [14].

Next, we analyze the local, or q-integrated imaginary part of the susceptibility, which is defined by

$$\chi''(\omega) = \frac{1}{4\pi^2}\int d^2q \ Im\Big\{\chi^{+-}(\mathbf{q},\mathbf{q},\omega)\Big\} \ . \tag{9}$$

In the low-frequency limit, we obtain

$$\chi''(\omega) = \frac{1}{\sqrt{2}c_{sw}\sqrt{1-2J'/J}}\Big[1+O\Big(\omega^2\Big)\Big] \tag{10}$$

Note that on the mean-field level, J' increases the overall scale of $\chi''(\omega)$ (this is opposite to the effect of quantum corrections, as we will discuss later). In Fig. 2 we present a fit of $\chi''(\omega)$ with $t' = -0.3$ to the experimental data from Ref. [4]. For this comparison we multiplied Eqs.(6) and (10) with $Z_d g^2\mu_B^2$, where g is the Landé-factor, μ_B is the Bohr magneton and Z_d represents the overall renormalization due to quantum fluctuations [10,11]. The inset shows the systematic evolution of $\chi''(\omega)$ with increasing t'/t. For $t' = 0$, $\chi''(\omega)$ is logarithmically divergent at the maximum magnon energy ω_{max} due to the degeneracy of the dispersion along the boundary of the MBZ. A finite t' removes this degeneracy (see Fig. 1) and transforms the divergence into a maximum which shifts to lower energies with increasing t'/t. We can identify three characteristic features of $\chi''(\omega)$, which in addition to c_{sw}, provide enough information to extract J' from the experimental data. These features are the position of the maximum, the cut-off energy, and the position of the jump, denoted by an arrow in Fig. 2. The cut-off energy is obviously given by the maximum magnon energy $\omega_{max} = 2J - 2J'$, but for small J' yields the same information as c_{sw}. To determine the position of the jump and the peak we observe that at higher frequencies $\chi''(\omega)$

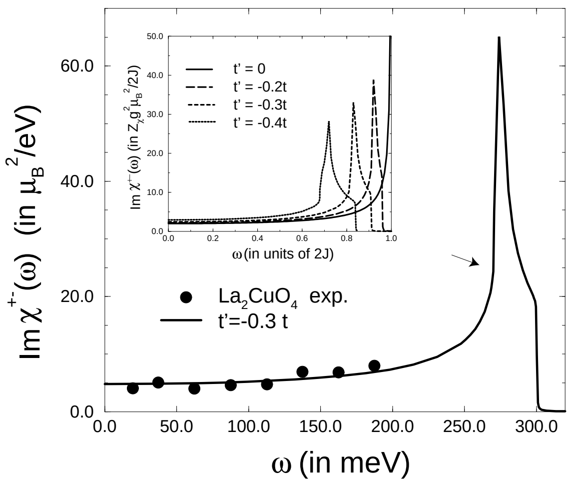

FIG. 2. Fit of the local susceptibility with $t' = -0.3t$ to the experimental data from Ref. [4]. The inset shows the systematic evolution of $\chi''(\omega)$ with increasing t'/t

reflects the density of states (DOS). It is then easy to check that the jump in $\chi''(\omega)$ arises from the excitation of magnons at $\mathbf{q} = (0, \pi)$ with energy $\omega_{\mathbf{q}} = 2J - 4J'$. Similarly, the peak in $\chi''(\omega)$ is determined by the flat maximum of the dispersion along the $(0, \pi)$ to (π, π) direction with energy

$$\omega_{peak} = 2J\sqrt{\frac{J - 2J'}{J + 2J'}} \; . \tag{11}$$

However, a fit of $\chi''(\omega)$ to the experimental data (Fig. 2) shows that the accessible energies are still about 75meV below any of these pronounced features, which makes it difficult to extract a precise value for J'.

We now turn to the analysis of the two-layer systems. The only change in our starting point Eq.(1) is the introduction of a hopping term $t_\perp$ between the planes. Diagonalizing the Hamiltonian as before, one obtains two valence and two conduction bands, whose dispersion is given by Eq.(2) with $\epsilon^-_{\mathbf{k}}$ replaced by $\epsilon^-_{\mathbf{k}} \pm t_\perp$. The subsequent calculation of the transverse susceptibilities is performed along the same lines as before, and has been reported earlier for $t' = 0$ [15]. Due to the coupling of the planes, one obtains a finite out-of-plane susceptibility with the two spins in Eq.(4) on different layers. The final result for the in-plane and out-of-plane susceptibilities in RPA approximation is given by

$$\chi^{+-}_{1,\alpha}(\mathbf{q},\mathbf{q},\omega) = -\frac{J\Big[1 - \nu_{\mathbf{q}} - \frac{J'}{J}(1 - cos(q_x)cos(q_y))\Big]}{\omega^2 - \omega^2_{opt}(\mathbf{q}) + i\delta}$$
$$\mp \frac{J\Big[1 - \nu_{\mathbf{q}} + \frac{J_\perp}{2J} - \frac{J'}{J}(1 - cos(q_x)cos(q_y))\Big]}{\omega^2 - \omega^2_{ac}(\mathbf{q}) + i\delta},$$
$$\chi^{+-}_{1,\alpha}(\mathbf{q},\mathbf{q}+\mathbf{Q},\omega) = -\frac{\omega}{2}\Bigg[\frac{1}{\omega^2 - \omega^2_{opt}(\mathbf{q}) + i\delta}$$
$$\pm \frac{1}{\omega^2 - \omega^2_{ac}(\mathbf{q}) + i\delta}\Bigg] \; , \tag{12}$$

where $\alpha = 1, 2$ (upper and lower sign), denotes the in-plane and out-of-plane susceptibilities, respectively. Note that $\chi(\mathbf{q}, \mathbf{q} + \mathbf{Q}, \omega)$ changes sign under the exchange of layers. The optical and acoustic magnon modes are doubly degenerate with dispersion

$$\omega_{ac,opt}(\mathbf{q}) = 2J\Bigg\{\Big[1 \mp \nu_{\mathbf{q}} + \frac{J_\perp}{2J} - \frac{J'}{J}(1 - cos(q_x)cos(q_y))\Big]$$
$$\times\Big[1 \pm \nu_{\mathbf{q}} - \frac{J'}{J}(1 - cos(q_x)cos(q_y))\Big]\Bigg\}^{1/2} \tag{13}$$

where the upper (lower) sign corresponds to the acoustic (optical) mode. The gap $\Delta = 2\sqrt{JJ_\perp}$ of the optical (or even) mode at $Q = (\pi, \pi)$ is not changed by J', however, the spin-wave velocity of the acoustic (or odd) mode is changed and now given by

$$c_{sw} = \sqrt{2}J\sqrt{1 - 2\frac{J'}{J}}\sqrt{1 + \frac{J_\perp}{4J}} \; . \tag{14}$$

It is important to note that since both Δ and c_{sw} are experimentally measured, J' does not only lead to a renormalization of J, but also of $J_\perp$. Using Eq.(14) one obtains (in the limit of small $J_\perp$)

$$J_\perp = \frac{\sqrt{2}}{c_{sw}}\sqrt{1 - 2\frac{J'}{J}}\Big(\frac{\Delta}{2}\Big)^2 \tag{15}$$

Using $t' = -0.45t$, we obtain from a fit of Eq.(13) to the experimental data [4], $J = 163$ meV, $J' = 33$ meV, and $J_\perp = 8.4$ meV. The value for J is about 30% larger, and the value for $J_\perp$ about 25% smaller than the ones reported in Ref. [4]. It is interesting that the different values for t' in La_2CuO_4 and $YBa_2Cu_3O_{6.15}$ lead to almost identical values for the nearest-neighbor exchange constants, in contrast to the results in Ref. [4].

In Fig. 3 we present a fit of the local susceptibility in the even and odd channel, $\chi''_{even,odd}(\omega) = \chi''_{11} \pm \chi''_{12}$, to the experimental data. The fit in both channels is quite good, though the scattering of the data is rather large. A finite t' again transforms the divergence of $\chi''(\omega)$ at ω_{max} into a maximum. Note, that the two maxima in $\chi''_{even,odd}$ do not occur at the same frequency, but are shifted by a finite amount $\Delta\omega = 2J_\perp(J'/J)/\sqrt{1 - (2J'/J)^2} \approx 3$meV. As before in the case of a single-layer, one can use the position of the jump and the maximum together with the value for c_{sw} to extract J'. However, as a comparison of χ'' for $J' = 0$ (dashed line) shows, the experimental data have to be extended to higher frequencies before one can extract J'.

Furthermore, using the data in Figs. 2 and 3 we compared the local in-plane susceptibility $\chi''_{11}(\omega)$ in $YBa_2Cu_3O_{6.15}$ and La_2CuO_4. We obtain that for $\omega < \Delta = 72$ meV, $\chi''_{11}(\omega)$ in $YBa_2Cu_3O_{6.15}$ is only half as

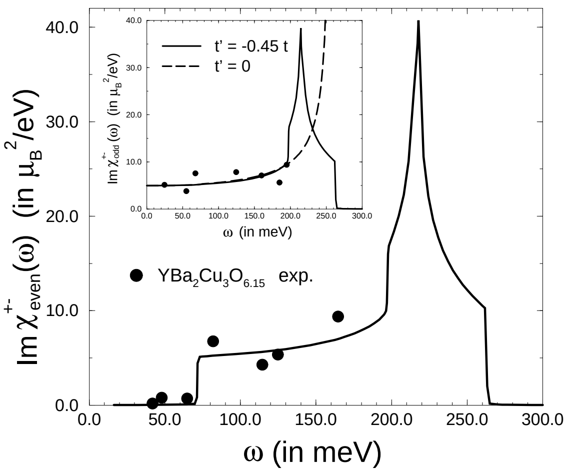

FIG. 3. The local susceptibility as a function of ω for the even channel and (see inset) the odd channel. The solid line corresponds to $t'/t = -0.45$, whereas the dashed line shows the result for $t'/t = 0$. The experimental data are taken from Ref. [4].

large as in La_2CuO_4, which is expected since the optical mode is gaped out. For 72 meV $< \omega$, the optical magnons in $YBa_2Cu_3O_{6.15}$ can be excited and χ''_{11} in both materials is approximately the same.

Finally, we consider quantum corrections in the presence of J'. A convenient way to calculate these corrections is to perform a systematic $1/S$-expansion in the Heisenberg model, as was done for the case $J' = 0$ in Ref. [11]. Considering a finite J' we performed calculations analogous to [11]. To lowest order in $1/S$, i.e., on the mean-field level, we recover as expected Eqs.(6) and (7). The next order $1/S$ corrections, which appear due to the normal ordering of quartic operator terms yield the following renormalizations (for $J'/J = 0.09$)

$$\tilde{J} = \left(1 + \frac{0.157}{2S}\right) J\,, \quad \tilde{J}' = \left(1 - \frac{0.123}{2S}\right) J'\,,$$
$$\tilde{c}_{sw} = \left(1 + \frac{0.188}{2S}\right) c_{sw}\,, \quad Z_d = 1 - \frac{0.454}{2S}\,. \qquad (16)$$

Comparing these results with the case $J' = 0$, we find that the spin-wave velocity is only slightly increased whereas Z_d is decreased by about 10%. Can these results explain the strong renormalization of χ'' observed experimentally ? A fit of $\chi''(0) = Z_d g^2 \mu_B^2/\sqrt{2}\tilde{c}_{sw}$ to the experimental data [4] showed, that the overall renormalization $Z_d^{exp} = 0.36$ of the dynamical spin susceptibility in La_2CuO_4 was much larger than the theoretical value $Z_d = 0.607$ obtained in the case $J' = 0$ [11]. For $J' \neq 0$ the overall renormalization of χ'' is given by a classical contribution, $1/\sqrt{1 - 2\tilde{J}'/\tilde{J}}$, and the quantum corrections Z_d, which means that Z_d^{exp} should be compared with $Z' = Z_d/\sqrt{1 - 2\tilde{J}'/\tilde{J}}$. Here we use the renormalized $\tilde{J}, \tilde{J}'$ and $\tilde{c}_{sw}$, since only these are experimentally measurable. With $\tilde{J}'/\tilde{J} = 0.09$, which neglecting small corrections to order $(1/S)^2$ [11] implies $J'/J = 0.126$, we obtain $Z' = 0.57$. Though this value is only about 6% smaller than the one in Ref. [11], it shows that a finite J' leads to an improved agreement with the experimental data.

In conclusion we have provided a detailed study of the effects of t', and consequently J', on the spin dynamics in single and double-layer systems. We have shown that J' changes the value for J and $J_\perp$ extracted from the experimental data, yielding two almost identical values for J in $YBa_2Cu_3O_{6.15}$ and La_2CuO_4. We demonstrated that the changes due to J' in the high frequency structure of $\chi''(\omega)$ provide the possibility to extract values for the exchange constants. Precise results, however, will require a higher accuracy of the INS data and their extension to higher frequencies. Furthermore, we obtained that J' leads to stronger quantum corrections. Finally, it was recently pointed out that the ^{17}O NMR signal in Ni doped $YBa_2Cu_3O_{6+x}$ is sensitive to the momentum structure of $\chi'(\mathbf{q})$ [16]; an effect which might be used to detect changes in $\chi'(q)$ due to J'. Further quantitative studies in this direction are clearly called for.

We would like to thank A.V. Chubukov, S. Hayden, D. Pines, A. Sandvik, J. Schmalian and C. Slichter for valuable discussions. This work has been supported in part by the Science and Technology Center for Superconductivity through NSF-grant DMR91-20000.

[1] D. Pines, Z. Phys. B **103**, 129 (1997).
[2] D. J. Scalapino, Phys. Rep. **250**, 329 (1995).
[3] K.B. Lyons, P.A. Fleury, L.T. Schneemeyer, and J.V. Waszczak, Phys. Rev. Lett. **60**, 732 (1988).
[4] S. M. Hayden *et al.*, preprint, cond-mat 9710181.
[5] P. Bourges, H. Casalta, A.S. Ivanov. and D. Petitgrand, Phys. Rev. Lett. **79**, 4906 (1997).
[6] D. Duffy and A. Moreo, Phys. Rev. B **52**, 15607 (1995).
[7] A.V. Chubukov and K. Musaelian, J. Phys. Cond. Mat. **7**, 133 (1995).
[8] B.O. Wells *et al*, Phys. Rev. Lett. **74**, 964 (1995).
[9] M. S. Hybertsen, E. B. Stechel, M. Schluter, and D. R. Jennison, Phys. Rev. B **41**, 11068 (1990).
[10] R.R.P. Singh, Phys. Rev. B **39**, R9760 (1989).
[11] J. Igarashi, Phys. Rev. B **46**, 10763 (1992).
[12] J.R.Schrieffer, X.G.Wen, and S.C.Zhang, Phys. Rev. B **39**, 11663 (1989); A.V.Chubukov and D.M.Frenkel, Phys. Rev. B **46**, 11884 (1992).
[13] P.W. Anderson and J.R. Schrieffer, Phys. Today **44**, 55 (1991).
[14] S. M. Hayden *et al.*, Phys. Rev. Lett. **67**, 3622 (1991).
[15] D.K. Morr, A.V. Chubukov, A. Kampf, and G. Blumberg, Phys. Rev. B **54**, 3468 (1996).
[16] J. Bobroff *et al.*, Phys.Rev. Lett. **79**, 2117 (1997); D. Morr *et al.*, to appear in Phys. Rev. Lett.